Physica E 44 (2012) 2021–2026

Contents lists available at SciVerse ScienceDirect

Physica E

journal homepage: www.elsevier.com/locate/physe

Electromechanical switch in metallic graphene nanoribbons via twisting

Hong Li [a,b], Nabil Al-Aqtash [b], Lu Wang [b], Rui Qin [a], Qihang Liu [a], Jiaxin Zheng [a], Wai-Ning Mei [b], R.F. Sabirianov [b], Zhengxiang Gao [a], Jing Lu [a,*]

[a] State Key Laboratory of Mesoscopic Physics and Department of Physics, Peking University, Beijing 100871, PR China
[b] Department of Physics, University of Nebraska at Omaha, Omaha, NE 68182-0266, USA

HIGHLIGHTS

- Twisting a metallic ferromagnetic ZGNR is a possible way to make an electromechanical switch.
- Twisting would cause orbital symmetry mismatch of the two leads in a symmetric ferromagnetic ZGNR.
- Zero transmission gap is thus generated, and hence the current is suppressed.
- The switch series can be obtained *via* multiply overturning the nanoribbon.

GRAPHICAL ABSTRACT

We propose a novel electromechanical switch *via* twisting a metallic ferromagnetic symmetric zigzag-edged graphene nanoribbon. The switch realizes a spin valve function in a flexible nanoribbon by twisting in addition to change in the magnetic field direction.

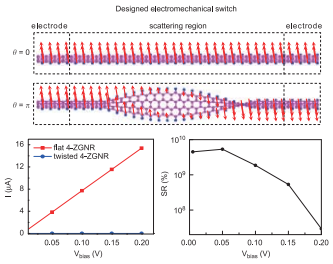

ARTICLE INFO

Article history:
Received 28 January 2012
Received in revised form
16 May 2012
Accepted 6 June 2012
Available online 15 June 2012

ABSTRACT

We imposed screwing operation to a metallic ferromagnetic zigzag-edged graphene nanoribbon (ZGNR) with a narrow width and a finite length, and the polarized charge transport is investigated by using Nonequilibrium Green's function in combination with density functional theory. The current are nearly completely suppressed when the ZGNRs are overturned. Inspiringly, this metal-to-semiconductor transition tuned by screwing operation is reversible. Hence our investigation brings forward a novel electromechanical switch, and such a switch is equivalent to a spin valve without resort to an external magnetic field.

1. Introduction

The components (e.g., field effect transistor) that can be converted controllably and reversibly between the high- and low-resistance states are the building blocks of the modern electronics. The modern electronics are based on the semiconducting silicon as the current through it can be easily tuned by the electric field. As the performance improvements of silicon are nearing the limits, new materials and mechanism are constantly searched for. In 2004, Geim et al. [1] fabricated all-metallic field effect transistors out of metallic atomically thin graphene films for the first time as graphene is thin enough to avoid the electric field screen. Compared to traditional semiconducting devices, the all-metallic ones could be scaled down to much smaller sizes and would consume less energy and operate at higher frequencies. Besides, graphene has a much higher mobility [1–4] (10^4–10^5 $cm^2/V\,s$) than silicon, suggestive of a quicker switch speed of the devices.

Besides extraordinary electronic property, graphene also has an extraordinary mechanical property. The C–C bonds breaking strength is the largest ever measured, while it is very flexible out-of-plane [5]. In addition, it can be well restored even after released from up to 20% stretching [6]. However, it is extremely difficult to open a band gap in graphene *via* mechanical methods

* Corresponding author.
E-mail address: jinglu@pku.edu.cn (J. Lu).

1386-9477/$ - see front matter © 2012 Elsevier B.V. All rights reserved.
http://dx.doi.org/10.1016/j.physe.2012.06.004

such as uniaxial strain and bending [6,7]. Graphene nanoribbons (GNRs) have interesting chirality dependent electronic and magnetic properties [8,9]. The ground states of the armchair-edged GNRs (AGNRs) and the zigzag-edged GNRs (ZGNRs) are nonmagnetic semiconductors and antiferromagnetic semiconductors, respectively. Both the ferromagnetic (a slightly higher in energy than the ground state) and the nonmagnetic states of ZGNRs are metallic. Semiconducting AGNRs are sensitive to mechanical operations [7,10–13], whereas metallic nonmagnetic ZGNRs are rather robust to mechanical operations. Uniaxial strain [7,11], shear strain [7], step-shaped [13], arched deformation [13], and folded deformation [10] cannot change the metallic behavior of nonmagnetic ZGNRs at all.

Twisting is a specific deformation unique to nanoribbons. Twisted GNRs [14] and MoS_2 [15] and WS_2 [16] nanoribbons have been observed experimentally. Very recently, first principles calculations show that twisting can close the band gap of specific semiconducting AGNRs [17–19]. An interesting question arises: Is it possible to transform metallic ZGNRs to semiconducting ones by twisting way?

In this paper, we present ab initio quantum transport study on the twisting effects on metallic ZGNRs. Intriguingly, the currents of the ferromagnetic metallic ZGNRs with axial symmetry can be fully turned off via twisting. Therefore, a novel electromechanical switch mode, which is unique to nanoribbons, is revealed. The operation mechanism is equivalent to a kind of spin valve.

2. Model and method

We use *N*-ZGNR to denote an H-passivated ZGNR with *N* zigzag chains across the width, and several *N*-ZGNRs (N=4–8) with a width range of 0.93–1.78 nm are studied. Both the metallic nonmagnetic and ferromagnetic states are considered. Successive screw operations about the axis of the ZGNRs are imposed as indicated in Fig. 1a. We define a twist angle φ as the relative rotation angle of two adjacent atom lines. The C–C bonds are elongated after twisting, and the outermost bonds endure the largest strain. We take $\varphi=5^\circ$ for all the ribbons unless otherwise specified, and the maximum strain is still below the breaking strength. Seamless devices are constructed for *N*-ZGNRs (N=4–8). We establish a two-probe model to study the transport properties. Fig. 1b and c is the schematic of the two-probe model based on a ferromagnetic flat and once overturned 4-ZGNR, respectively, where the red arrows represent the spin orientation. For once overturned ZGNR, the scattering region contains 18 twisted unit cells, and there are 4 flat unit cells as buffer regions to connect the electrodes. The total length of the central region is 6.40 nm. Twice and thrice overturned 4-ZGNRs with different flat intervals (namely, interval between two screw operations on the ZGNR) are also considered. The total lengths of central regions of these structures are 10.83–21.16 nm. We use the symbol (θ, l) to denote a 4-ZGNR with an overturning angle of θ and a flat interval of l. Fig. 1d and e shows two twisted configurations with $\theta=2\pi$ and l=2.95 nm (denoted as (2π, 2.95 nm)) and $\theta=3\pi$ and l=2.95 nm (denoted as (3π, 2.95 nm)), respectively. Apparently, the once overturned ZGNR has $\theta=\pi$ and l=0 nm.

We calculate the electronic properties of the infinite ferromagnetic ZGNRs by using the density functional theory (DFT) implemented in the ATK 2008.10 code [20,21]. The charge transport of the finite nonmagnetic ZGNRs and ferromagnetic ZGNRs with collinear spin configurations is calculated by using the DFT coupled with nonequilibrium Green's function (NEGF) method also implemented in the ATK 2008.10 code. The spin flip processes are supposed to be negligible in the collinear calculations. We choose the generalized gradient approximation (GGA) of

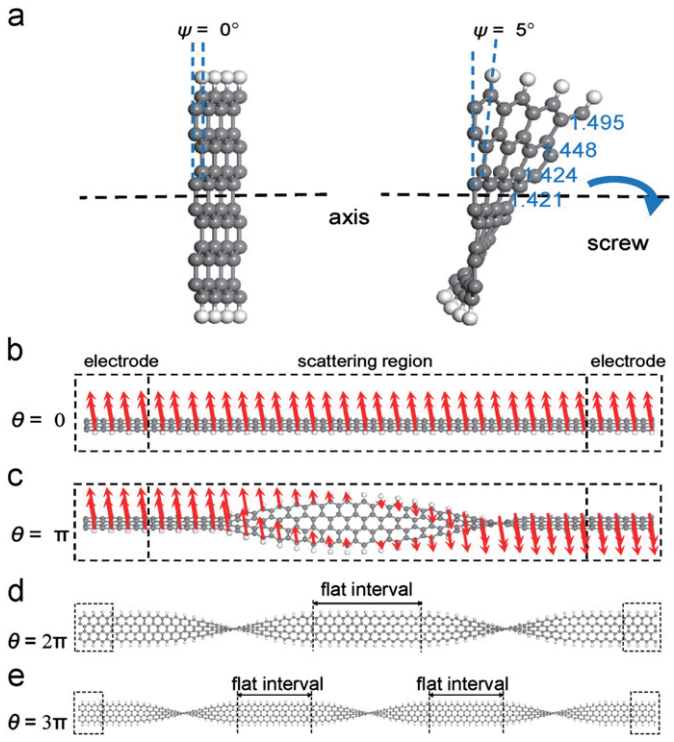

Fig. 1. (Colors online) (a) Illustration of screw operation on a 6-ZGNR. The elongated bond lengths from its original 1.421 Å are marked. (b) and (c) A ferromagnetic 4-ZGNR based device with the hypothetical spin switching process indicated by the red arrows. Schematic model of a twice overturned 4-ZGNR with a flat interval of 2.95 nm (c) and a thrice overturned 4-ZGNR with two flat intervals of 2.95 nm (d). Gray ball: C; white ball: H. (For interpretation of the references to color in this figure caption, the reader is referred to the web version of this article.)

Perdew–Burke–Ernzerhof (PBE) form [22] as the exchange-correlation functional, and we use a single-ζ basis set (SZ) and a mesh cut-off energy of 150 Ry in all the above calculations. The Monkhorst–Pack [23] *k*-points meshes of the infinite ZGNR and the electrodes of the devices are set to $1\times1\times29$ and $1\times1\times500$, respectively. The electron temperature is set as 300 K. We also have considered a single-ζ polarization basis set (SZP) for a twisted 4-ZGNR with $\varphi=10^\circ$ (the twisted part contains nine unit cells), and the current obtained does not change much compared to that with a SZ basis set. So it is with tested mesh cut-off energy of 300 Ry compared to that with 150 Ry (see Table S1 in the Supporting Information).

The spin-resolved current $I_\sigma(V_{\rm bias})$ under a finite bias of $V_{\rm bias}$ is calculated using the Landauer–Büttiker formula [24]

$$I_\sigma(V_{\rm bias})=\frac{e}{h}\int_{-\infty}^{\infty}\{T_\sigma(E,V_{\rm bias})[f_{\rm L}(E-\mu_{\rm L})-f_{\rm R}(E-\mu_{\rm R})]\}\,dE \quad (1)$$

where $T_\sigma(E,V_{\rm bias})$ is the transmission probability, $f_{\rm L/R}$ is the Fermi–Dirac distribution function for the left (L)/right (R) electrode, $\mu_{\rm L}/\mu_{\rm R}$ is the electrochemical potential of the L/R electrode, and σ is a spin index. The total current $I(V_{\rm bias})$ is the sum of the two spins' currents.

To check the effects of the structural relaxation on the results, we select the structure of a twisted 4-ZGNR with $\varphi=10^\circ$ to relax. The four flat unit cells as buffer regions are fixed during the relaxation to keep the helical twist angle. The structure is optimized by using the all-electron double numerical atomic orbital basis set (DN) implemented in the $DMol^3$ package [25], and the convergence criterion of the maximum atomic force is 0.03 eV/Å. The GGA of PBE form [22] is used for the exchange-correlation functional. The current obtained in this optimized

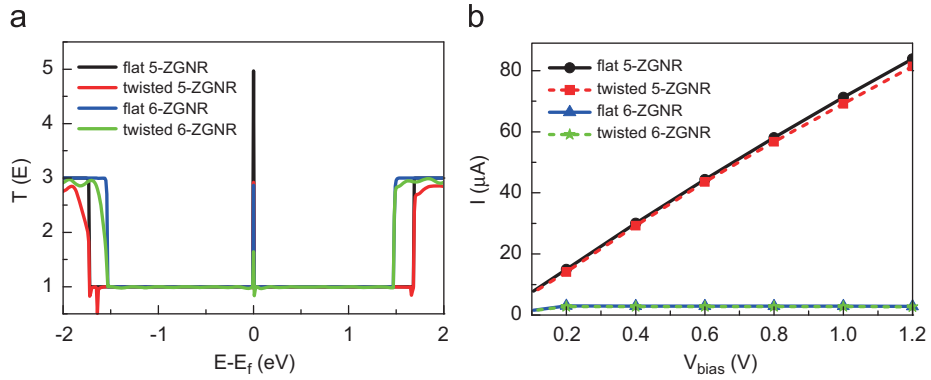

Fig. 2. (a) Transmission spectra at zero bias and (b) the I–V_{bias} characteristics of the nonmagnetic 5- and 6-ZGNR.

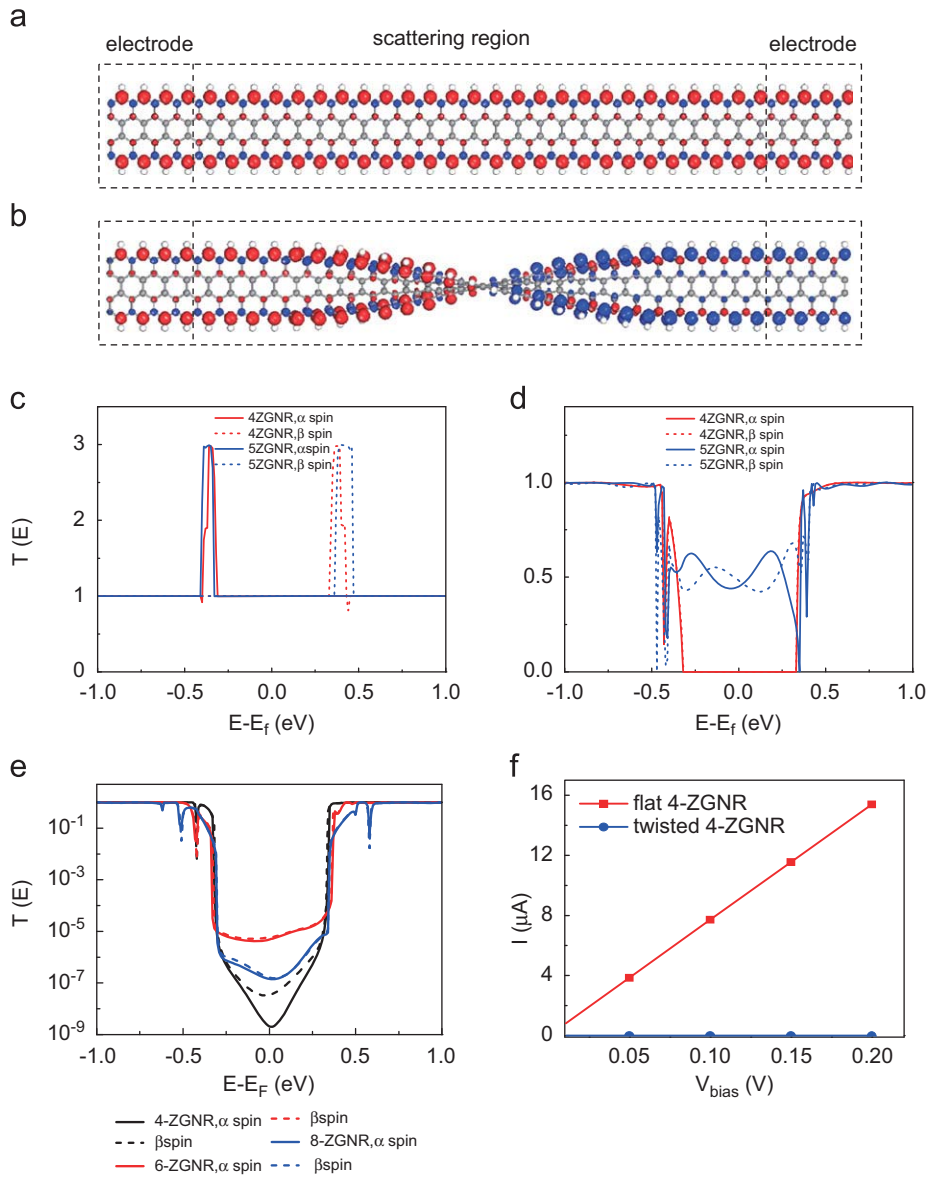

Fig. 3. (Colors online) Calculated collinear spatial spin density distributions of the flat (a) and once overturned (b) ferromagnetic 4-ZGNR. The spin density disappears in the middle of the overturned 4-ZGNR as the destructive overlap between opposite spins. Red and blue are used to denote the spin-up and spin-down orientations, respectively. The isovalue is 0.01 a.u. Gray ball: C; white ball: H. Spin-resolved transmission spectra at zero bias of the flat (c) and once overturned (d) ferromagnetic 4-ZGNR and those of the flat and once overturned ferromagnetic 5-ZGNR. (e) Spin-resolved transmission spectra at zero bias of the once overturned ferromagnetic N-ZGNRs (N=4, 6, and 8) on the logarithmic coordinate system. (f) I–V_{bias} characteristics of the flat and once overturned ferromagnetic 4-ZGNR. (For interpretation of the references to color in this figure caption, the reader is referred to the web version of this article.)

structure does not change much compared with that of an unoptimized one (see Table S1 in the Supporting Information). Thus the structures used in this paper are not optimized.

3. Results and discussion

The transmission spectra at zero bias and the I–V_{bias} characteristics of the nonmagnetic 5- and 6-ZGNR are given in Fig. 2a and b, respectively. The transmission spectra are almost unchanged after twisting except for a decrease at the Fermi level (E_f) for both nonmagnetic 5- and 6-ZGNR. And the currents exhibit only tiny decrease within $V_{bias}=1.2$ V. Hence the twisting deformation cannot tune the conductive transport properties of the nonmagnetic ZGNRs. Then we will focus on the twist effects on the ferromagnetic ZGNRs with collinear spin configurations.

Table 1
Zero transmission gaps (eV) of α/β spins as a function of the ribbon width and bias voltage.

Bias (V)	Ribbon		
	4-ZGNR	6-ZGNR	8-ZGNR
0	0.64/0.64	0.67/0.67	0.62/0.62
0.005	0.66/0.64	0.69/0.67	0.64/0.64
0.05	0.72/0.62	0.74/0.64	0.70/0.60
0.1	0.76/0.56	0.79/0.59	0.74/0.54
0.15	0.79/0.50	0.82/0.54	0.79/0.50
0.2	0.86/0.47	0.89/0.49	0.84/0.45
0.3	0.96/0.45	0.99/0.40	–
0.4	1.06/0.38	1.09/0.30	–
0.6	1.24/0.27	–	–

The calculated spatial spin densities of the flat and once overturned ferromagnetic 4-ZGNRs are given in Fig. 3a and b, respectively. The spin density of the flat ribbon is uniform along its length. The screw operation makes the spin direction of the two leads antiparallel, and only a single-atom-layer Domain Wall (DW) is generated in the interface as the destructive overlap between opposite spins in the two leads in the collinear model. The single DW was also found in the spin valve model based on ferromagnetic ZGNRs with collinear spin configurations [26], which works *via* changing the relative direction of the local magnetic field applied on the two electrodes. The spin-resolved transmission spectra of the flat ferromagnetic 4- and 5-ZGNR at zero bias have conventional perfect transmission as shown in Fig. 3c. After twisting, a remarkable zero transmission gap (ZTG) appears around E_f in the ferromagnetic 4-ZGNR with a width of 0.64 eV. By contrast, the transmission coefficients are only decreased by about half around E_f in the ferromagnetic 5-ZGNR as shown in Fig. 3d.

The spin-resolved transmission spectra at zero bias of the once overturned ferromagnetic N-ZGNRs ($N=4$, 6, and 8) on the logarithmic coordinate system are given in Fig. 3e. The ZTG is also available around E_f for the 6- and 8-ZGNR with widths of 0.67 and 0.62 eV, respectively. The total transmission coefficients at E_f of the 4-, 6-, and 8-ZGNR are 3.68×10^{-8}, 1.07×10^{-5}, and 3.06×10^{-7}, respectively. Fig. 3f gives the currents of the flat 4-ZGNR and its twisted counterpart from $V_{bias}=0$–0.2 V. The current in the flat ribbon I_{flat} is significantly larger than its counterpart in the twisted ribbon I_{twist} and increases linearly with the bias voltage. This is because the transmission probability remains to be one around the E_f in the flat ribbon as the bias increases from 0 to 0.2 V, while the ZTG remains in its twisted counterpart (see Fig. S1 in Supporting Information). The ZTGs of

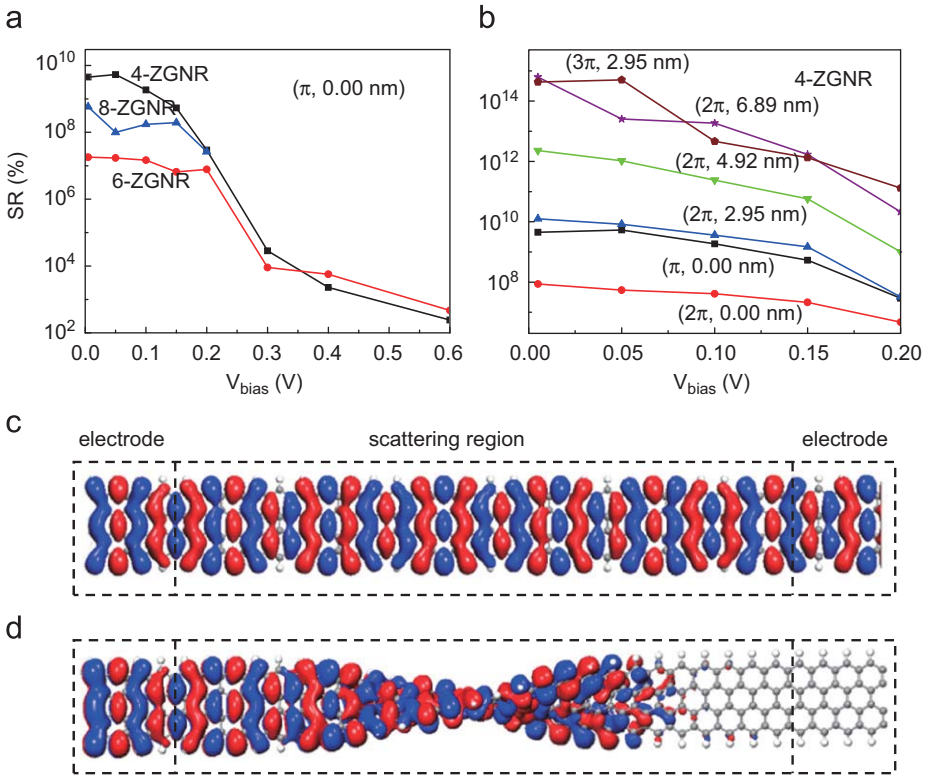

Fig. 4. (Colors online) Electromechanical switch ratios as a function of bias voltage of the ferromagnetic N-ZGNRs ($N=4$, 6, and 8) with once overturning (a) and 4-ZGNRs with different overturning angles and flat intervals (b). The α spin transmission eigenchannels at the Γ points at the Fermi level of the flat (c) and once overturned (d) 4-ZGNR. The isovalue is 0.02 a.u. Red and blue are used to indicate the positive and negative signs of the wavefunctions, respectively. Gray ball: C; white ball: H. (For interpretation of the references to color in this figure caption, the reader is referred to the web version of this article.)

α/β spins as a function of the ribbon width and bias voltage are summarized in Table 1.

We define the electromechanical switch ratio as SR=(I_{flat}–I_{twist})/I_{twist}. Ultra high SRs of the once overturned ferromagnetic *N*-ZGNRs (*N*=4, 6, and 8) as a function of the bias voltage are shown in Fig. 4a. The SRs generally decrease with the increasing bias. At a given bias, the SRs increase in the orders of 6-, 8-, and 4-ZGNR, which are consist with the decreasing orders of the transmission coefficients around E_f in the twisted ribbons. The maximum SRs of the 4-, 6-, and 8-ZGNR are 5.3×10^{9}% (at V_{bias}=0.05 V), 1.8×10^{7}% (at V_{bias}=0.005 V), and 5.8×10^{8}% (at V_{bias}=0.005 V), respectively, and the SRs decline to 2.9×10^{7}%, 7.8×10^{6}%, and 2.6×10^{7}% at V_{bias}=0.2 V, respectively. The maximum SRs obtained here are comparable to the maximum magnetoresistance obtained in the ferromagnetic ZGNR-based spin valve models [26,27]. The SRs of over 10^{3}% are obtained in both 4- and 6-ZGNR at V_{bias}=0.4 V and they both decrease by about one order of magnitude at V_{bias}=0.6 V. The SRs as a function of the ribbon width and bias voltage are summarized in Table 2. We also calculate the SRs at V_{bias}=0.005 V of the once overturned 4-ZGNRs with a twist angle of $\varphi=3^{\circ}$ and $\varphi=10^{\circ}$, and the values are 1.5×10^{6}% and 6.6×10^{5}%, respectively, as given in Fig. S2. The calculated SRs of the ferromagnetic 5- and 7-ZGNR at V_{bias}=0.005 V are only SRs=145% and 40%, respectively, because of a small reduction in the transmission coefficients around E_f upon twisting.

Table 2
Switch ratios as a function of the ribbon width and bias voltage.

Bias (V)	Ribbon		
	4-ZGNR (%)	6-ZGNR (%)	8-ZGNR (%)
0.005	4.50×10^{9}	1.80×10^{7}	5.77×10^{8}
0.05	5.34×10^{9}	1.71×10^{7}	9.91×10^{7}
0.1	1.86×10^{9}	1.47×10^{7}	1.74×10^{8}
0.15	5.33×10^{8}	1.65×10^{7}	1.94×10^{8}
0.2	2.93×10^{7}	7.80×10^{6}	2.62×10^{7}
0.3	2.86×10^{4}	9.02×10^{4}	–
0.4	2.27×10^{3}	5.70×10^{3}	–
0.6	2.44×10^{2}	4.72×10^{2}	–

The switch series can be obtained *via* multiply overturning the nanoribbon. Fig. 4b shows the SRs of the ferromagnetic 4-ZGNR with different overturning angles and flat interval as a function of the bias voltage. The SRs also generally decrease with the increasing bias for all the switches. With the same length of flat interval *l*=2.95 nm, the SR of the thrice overturned 4-ZGNR are great higher than that of a twice overturned one at a given bias. For example, the SR at V_{bias}=0.005 V in twice overturned 4-ZGNR is 1.3×10^{10}%, and it increases to 4.3×10^{14}% in the thrice overturned one. We also investigate the effect of the flat interval length in the twice overturned 4-ZGNR, and we find that the longer the flat interval, the larger the SR. For example, the SR at V_{bias}=0.005 V in the twice overturned 4-ZGNR monotonically increases from 8.7×10^{7}% to 6.3×10^{14}% with *l* increases from 0 to 6.89 nm. In all, the SR can be further enhanced *via* multiply overturning, and the larger the overturning angle and the flat interval, the larger the SR. This is because that the flat interval serves as a virtual electrode to some extent, and the longer the flat interval, the closer the virtual electrode to the real electrode. This is equivalent to two switches in series.

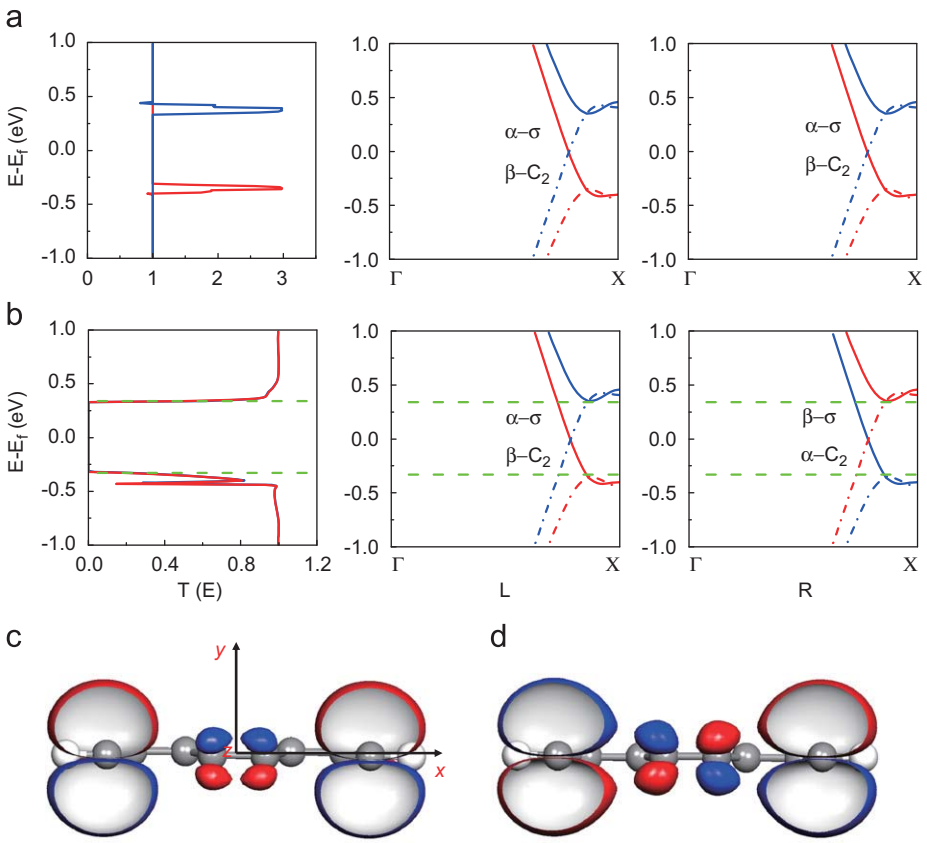

Fig. 5. (Colors online) Spin-resolved transmission spectra and band structures of the left (L) and right (R) leads for the ferromagnetic flat (a) and once overturned (b) 4-ZGNR. The wavefunctions at the X points of the σ (c) and C_2 (d) bands. The isovalue is 0.04 a.u. Red and blue are used to indicate the positive and negative signs of the wavefunctions, respectively. The coordinate system is shown in (c). Gray ball: C; white ball: H. (For interpretation of the references to color in this figure caption, the reader is referred to the web version of this article.)

The α spin transmission eigenchannels at the Γ points at the E_f of the flat and once overturned 4-ZGNR are given in Fig. 4c and d, respectively. We can see that the wave function of the flat 4-ZGNR is uniform, while that of its twisted counterpart is totally cut-off (but not in the DW region) before it can reach to the right lead. The transmission eigenvalue of the flat 4-ZGNR is 1.00 and means that the incoming wave function is not scattered at all and all of the incoming wave is able to reach the other lead. This leads to the conventional perfect transmission coefficient at E_f in the flat ribbon. On the other hand, the transmission eigenvalue of the once overturned 4-ZGNR is only 1.82×10^{-9}, which means that the incoming wave function is totally scattered and the incoming wave is not able to reach the other lead at all. This leads to the tiny transmission coefficient at E_f in the twisted nanoribbon. The β spin transmission eigenchannels are the same (not shown).

To interpret the origin of the giant SRs, we have calculated the band structures at zero bias of the two leads for the flat and twisted 4-ZGNR as shown in the central and right panels of Fig. 5a and b, respectively. There are two bands that contribute to the transmission spectra around E_f. The spin orientation of the two bands are different, and the two bands have distinct definite parity under the *yz* midplane mirror operation, which are odd (σ symmetry) and even parity (C_2 symmetry), respectively (labeled in the bands). Fig. 5c and d shows the wavefunctions at the *X* points of the σ and C_2 bands, respectively. In the flat nanoribbon, the electrons with α and β spin orientation of both the two leads have σ and C_2 symmetry, respectively. Therefore, electrons transfer smoothly from the left lead to the right lead, thus this constructive matching yields perfect transmission around E_f and thus high current. Whereas in the ZTG region of the overturned nanoribbon, due to the overturning of the spin direction, the bands of the left and right lead are either mismatched in the spin or in the symmetry and thus electrons from the left lead cannot transfer to the right lead. The orbital mismatch mechanism is absent in the ZGNRs without axial symmetry, this is why the SR obtain in the ferromagnetic 5-ZGNR is only 145% at $V_{bias}=0.005$ V, severely smaller than that of the ferromagnetic 4-ZGNR with a value of 4.5×10^{9}%. The mechanism to generate the ZTG in ferromagnetic metallic ZGNRs with axial symmetry *via* twisting is identical to that of the proposed spin valve where the ZTG is opened by applying contrary magnetic fields on the two leads of ZGNRs.

To fabricate the electromechanical switch, there are two issues to figure out at first. The first is to obtain of a symmetric ZGNR with ferromagnetic state. Very recently, bottom-up fabrication of atomically precise GNRs has been achieved in labs [28]. This provides a route to enable GNRs with engineered electronic and magnetic properties. The second is to realize the controllable screw operation on ZGNRs. Controllable stretching and bending graphene are already actualized in labs [5,6], and we believe that there is a possibility to realize screw operation on GNRs some day.

4. Conclusion

In conclusion, we propose a novel electromechanical switch *via* twisting a metallic ferromagnetic symmetric ZGNR from ab initio quantum transport calculations. The switch ratios of our switches are giant, and can be furthermore enhanced *via* multiply overturning. This controllable and reversible metallic-to-semiconductor transition is kind of inspiring to realize all-metallic devices. Our work also suggests that a spin valve function in a flexible symmetric ZGNR with ferromagnetic state can be realized by twisting in addition to change in the magnetic field direction.

Acknowledgments

This work was supported by the NSFC (Grant Nos. 90206048, 20771010, 10774003, 90606023, and 20731160012), National 973 Projects (Nos. 2006CB932701, 2007AA03Z311, and 2007CB936200, MOST of China), Fundamental Research Funds for the Central Universities, National Foundation for Fostering Talents of Basic Science (No. J0630311), Program for New Century Excellent Talents in University of MOE of China, and Nebraska Research Initiative (No. 4132050400) of USA. H. Li acknowledges also the financial support from the China Scholarship Council.

Appendix A. Supporting information

Supplementary data associated with this article can be found in the online version at doi:10.1016/j.physe.2012.06.004.

Test currents of an optimized once overturned 4-ZGNRs (opt) and unoptimized once overturned 4-ZGNRs (unopt) with more accurate basis sets and cut-off energy, spin-resolved transmission spectra at bias voltages of 0, 0.05, and 0.1 V for the flat and once overturned *N*-ZGNRs ($N=4$, 6, and 8), and electromechanical switch ratios at $V_{bias}=0.005$ V of the once overturned 4-ZGNRs with various twist angle φ. This material is available free of charge via the Internet at http://ees.elsevier.com/physe/.

References

[1] K.S. Novoselov, A.K. Geim, S.V. Morozov, D. Jiang, Y. Zhang, S.V. Dubonos, I.V. Grigorieva, A.A. Firsov, Science 306 (2004) 666.
[2] S.V. Morozov, K.S. Novoselov, M.I. Katsnelson, F. Schedin, D.C. Elias, J.A. Jaszczak, A.K. Geim, Physical Review Letters 100 (2008) 016602.
[3] A.K. Geim, K.S. Novoselov, Nature materials 6 (2007) 183.
[4] K.S. Novoselov, A.K. Geim, S.V. Morozov, D. Jiang, M.I. Katsnelson, I.V. Grigorieva, S.V. Dubonos, A.A. Firsov, Nature 438 (2005) 197.
[5] C. Lee, X. Wei, J.W. Kysar, J. Hone, Science 321 (2008) 385.
[6] K.S. Kim, Y. Zhao, H. Jang, S.Y. Lee, J.M. Kim, K.S. Kim, J.-H. Ahn, P. Kim J.-Y. Choi, B.H. Hong, Nature 457 (2009) 706.
[7] Y. Li, X. Jiang, Z. Liu, Z. Liu, Nano Res 3 (2010) 545.
[8] Y.-W. Son, M.L. Cohen, S.G. Louie, Nature 444 (2006) 347.
[9] Y.-W. Son, M.L. Cohen, S.G. Louie, Physical Review Letters 97 (2006) 216803.
[10] Y.E. Xie, Y.P. Chen, J. Zhong, Journal of Applied Physics 106 (2009) 103714.
[11] M. Poetschke, C.G. Rocha, L.E.F. Foa Torres, S. Roche, G. Cuniberti, Physical Review B 81 (2010) 193404.
[12] R. Rasuli, H. Rafii-Tabar, A.I. zad, Physical Review B 81 (2010) 125409.
[13] Z. Yu, L.Z. Sun, C.X. Zhang, J.X. Zhong, Applied Physics Letters 96 (2010) 173101.
[14] X. Li, X. Wang, L. Zhang, S. Lee, H. Dai, Science 319 (2008) 1229.
[15] Z. Wang, H. Li, Z. Liu, Z. Shi, J. Lu, K. Suenaga, S.-K. Joung, T. Okazaki, Z. Gu, J. Zhou, Z. Gao, G. Li, S. Sanvito, E. Wang, S. Iijima, Journal of the American Chemical Society 132 (2010) 13840.
[16] Z. Wang, K. Zhao, H. Li, Z. Liu, Z. Shi, J. Lu, K. Suenaga, S.-K. Joung, T. Okazaki, Z. Jin, Z. Gu, Z. Gao, S. Iijima, Journal of Materials Chemistry 21 (2010) 171.
[17] P. Koskinen, Applied Physics Letters 99 (2011) 013105.
[18] D. Gunlycke, J. Li, J.W. Mintmire, C.T. White, Nano Letters 10 (2010) 3638.
[19] D.-B. Zhang, T. Dumitrică, Small 7 (2011) 1023.
[20] M. Brandbyge, J.L. Mozos, P. Ordejon, J. Taylor, K. Stokbro, Physical Review B 65 (2002) 165401.
[21] J. Taylor, H. Guo, J. Wang, Physical Review B 63 (2001) 245407.
[22] J.P. Perdew, K. Burke, M. Ernzerhof, Physical Review Letters 77 (1996) 3865.
[23] H.J. Monkhorst, J.D. Pack, Physical Review B 13 (1976) 5188.
[24] S. Datta, Electronic Transport in Mesoscopic Systems, Cambridge University Press, Cambridge, England, 1995.
[25] B. Delley, Journal of Chemical Physics 92 (1990) 508.
[26] W.Y. Kim, K.S. Kim, Nature Nanotechnology 3 (2008) 408.
[27] R. Qin, J. Lu, L. Lai, J. Zhou, H. Li, Q. Liu, G. Luo, L. Zhao, Z. Gao, W.N. Mei, G. Li, Physical Review B 81 (2010) 233403.
[28] J. Cai, P. Ruffieux, R. Jaafar, M. Bieri, T. Braun, S. Blankenburg, M. Muoth, A.P. Seitsonen, M. Saleh, X. Feng, K. Mullen, R. Fasel, Nature 466 (2010) 470.